Clear-Sky Surface Solar Radiation During South China Sea Monsoon Experiment

Po-Hsiung Lin[1], Ming-Dah Chou[2], Qiang Ji[3], Si-Chee Tsay[2]

[1]Department of Atmospheric Sciences, National Taiwan University, Taipei, Taiwan.
[2]NASA/Goddard Space Flight Center, Greenbelt, Maryland.
[3] Science Systems and Applications, Inc., Lanham, Maryland.

To be April, 2000

Submitted to the Geophysical Research Letter

Abstract:

Downward solar fluxes measured at Dungsha coral island (20°42'N, 116°43'E) during the South China Sea Monsoon Experiment (May-June 1998) have been calibrated and compared with radiative transfer calculations for three clear-sky days. Model calculations use water vapor and temperature profiles from radiosound measurements and the aerosol optical thickness derived from sunphotometric radiance measurements at the surface. Results show that the difference between observed and model-calculated downward fluxes is <3% of the daily mean. Averaged over the three clear days, the difference reduces to 1%. The downward surface solar flux averaged over the three days is 314 Wm^{-2} from observations and 317 Wm^{-2} from model calculations. This result is consistent with a previous study using TOGA CAORE measurements, which found good agreements between observations and model calculations. This study provides an extra piece of useful information on the modeling of radiative transfer, which fills in the puzzle of the absorption of solar radiation in the atmosphere.

1. Introduction

The validity of radiation model calculations of atmospheric solar (shortwave, or SW) heating has long been an unsettled issue. Traditionally, this issue concerns primarily the excess atmospheric heating due to the presence of clouds that is not accounted for in radiation model calculations [*Cess et al.*, 1995; *Pilewskie and Valero*, 1995; *Ramanathan et al.*, 1995]. Other studies have shown that there is no clear evidence of the enhanced solar heating of the atmosphere due to clouds [*Imre et al.*, 1996; *Li et al.*, 1997]. Uncertainties in SW heating of both clear and cloudy skies could contribute to the uncertainty in the estimation of the cloud effect on atmospheric SW heating (or cloud radiative forcing, CRF). In a study of the global radiation data sets derived from surface measurements, satellite retrievals, and climate model simulations, *Arking* (1996) suggested that clouds had little effect on the solar heating of the atmosphere. Rather, the large atmospheric CRF of model calculations was caused by the underestimation of water vapor heating in clear atmospheres. Subsequently, there were a number of studies on the clear-sky solar heating of the atmosphere and the surface, which used various types of measurements (total, spectral, direct, diffuse radiation) at various geographical locations. Some studies have suggested that, for different reasons, radiation models highly underestimate the clear-sky atmospheric heating and, hence, overestimate the surface heating [*Kato et al.*, 1997; *Halthore, et al.*, 1998; *Arking*, 1999; *Pilewskie et al.*, 2000]. Other studies have found agreement between observations and model calculations [*Chou and Zhao*, 1997; *Conant et al.*, 1998; *Fu et al.*, 1998; *Mlawer et al.*, 2000]. Resolving this issue is very important because our ability to model the absorption of solar radiation affects the reliability of climate model simulations and remote sensing of a wide range of

geophysical parameters.

In May and June 1998, there was an intensive field experiment, South China Sea Monsoon Experiment, conducted in the South China Sea. The SCSMEX is an international field experiment to study physical processes and evolutions of the water and energy cycles of the East Asian monsoon system [*Lau et al.*, 2000]. There was a suite of instruments set up at Dungsha (20°42'N, 116°43'E) measuring surface radiation and atmospheric temperature, humidity, and aerosols. Dungsha is a small coral island with a length of ~1 km and a width of ~0.7 km. We use the data measured at Dungsha to study the surface SW radiation and compare the observations with radiation model calculations.

2. Surface Measurements and Radiative Transfer Model

Propagation of the East Asian summer monsoon (EASM) system during the spring-summer transition period influences the annual rainfall variation in the South China Sea. To understand the role of the EASM in the global energy and water cycle and to improve the simulation and prediction of East Asian monsoon and regional water resources, observations were conducted during two SCSMEX intensive observing periods (IOP). The first IOP was conducted in 5-25 May 1998 to observe atmospheric and oceanic circulation before the monsoon passing through the South China Sea. The second IOP was conducted in 5-25 June 1998 to observe tropical weather under the influence of EASM.

In addition to the weather stations operated by the Taiwanese navy, other advanced facilities were also operated on Dungsha during the SCSMEX IOP. These facilities included Australian C-band polarization radar system, remote pilot vehicle "Aerosonde", National Center for Atmospheric Research (NCAR) Integrated Sounding System (ISS),

and a NASA radiation measurement system. Radiative fluxes were measured in the period from 17 April through 6 July 1998. Three Epply Precision Spectral Pyranometers (PSP) and one Yankee Total Spectral Pyranometer were used to measure surface downward SW fluxes. The Epply pyranometers measured fluxes in the ultraviolet (0.3-0.4 μm), photosynthetically active radiation (0.4-0.7 μm), and infrared (0.7-2.8 μm) spectral bands. Two Epply Precision Infrared Radiometers (PIR) were used to measure the downward longwave fluxes. A CIMEL 318-1 sunphotometer and a Yankee six-band Multi-Filter Radiometer were used to measure direct- and sky-radiation. A single data-acquiring system processed and stored all radiative flux measurements with a one-minute sampling rate.

Except the CIMEL component, all of the radiation measurement facilities and the data acquiring system were new products with functions checked by the manufacturer in February 1998. After the SCSMEX campaign, all instruments were brought back to NASA/Goddard Space Flight Center for re-calibration. The pyranometer current equivalent to zero solar radiation was obtained by applying the dark-current checking procedure [*Ji and Tsay*, 2000]. The methodology involved the use of aluminum-made caps to cover the outer glass dome of the pyranometers during daytime operation. The overall uncertainty of the radiation measurements including data-logger performance is estimated to be 3%.

The aerosol optical thickness (AOT) was retrieved from the radiances measured by the Cimel Electronique CE318-1 automatic sun-tracking photometer. This instrument had seven filters centered at 340, 380, 440, 500, 675, 870, and 1020 nm. Two collimators with 1.2 degrees were used to measure direct- and sky-radiances every 15 min. The

measured-radiances were sent to the NASA Aerosol Network office [*Holben, et al.*, 1998] for AOT retrieval. The uncertainty of AOT under a clear-sky situation was estimated to be <0.01 for wavelengths >440 nm and <0.02 for shorter wavelengths.

Integrated Sounding System (ISS) GPS-based balloon sounding was launched twice a day at 0600 UTC and 1800 UTC. Vaisala RS80-15G radiosonde was used in this balloon sounding system to measure the atmospheric temperature and humidity profiles. The temperature sensor, THERMOCAP, has a 0.2% accuracy up to 50 hPa, and the humidity sensor, HUMICAP, has a 3% accuracy. It is found that the measured precipitable water agrees well with that retrieved from the Special Sensor Microwave Imager [*Wentz*, 1994] and the CIMEL radiance measurements at 940 nm.

We use the solar radiative transfer model (CLIRAD-SW) developed at the NASA Goddard Climate and Radiation Branch [*Chou and Suarez*, 1999] to compute the downward surface SW flux at Dungsha. The model has been applied to various atmospheric models used in the Goddard Laboratory for Atmospheres, including a general circulation model, a mesoscale model, and a cloud ensemble model. It includes the absorption due to water vapor, O_3, O_2, CO_2, clouds, and aerosols. Interactions among the absorption and scattering by clouds, aerosols, molecules (Rayleigh scattering), and the surface are fully taken into account. Fluxes are integrated virtually over the entire spectrum, from 0.175 μm to 10 μm. Integrated over all spectral bands and all absorbers, the surface heating is computed accurately to within a few watts per meter squared of high spectral-resolution calculations.

The pyranometer measurements of SW flux at Dungsha did not include radiation in the spectral region 2.8-10 μm. For comparisons between measured and computed surface

fluxes, radiation in this spectral region has to be taken into consideration. Line-by-line calculations show that the range of the surface flux in this spectral region is small. It ranges only from 10.8 W m^{-2} to 12.8 W m^{-2} for the column water vapor amount ranging from 2.8 cm to 5.6 cm when the sun is overhead. Therefore, we fit the surface flux computed for a column water vapor amount of 3 cm as a function of the solar zenith angle. The total flux computed using the SW radiation model is then reduced by an amount derived from this function to remove the radiation contained in the spectral region 2.8-10 μm.

3. Comparisons of measured and calculated surface SW fluxes

In the tropical western Pacific and the South China Sea, clouds are widespread, and it is difficult to identify those radiation measurements which are free of cloud influence. In studying the surface radiation in the Pacific warm pool during the Tropical Ocean and Global Atmosphere, Coupled Ocean-Atmosphere Response Experiment (TOGA COARE), *Chou and Zhao* [1997] used both the direct and diffuse components of the SW radiation to identify clear-sky surface fluxes. It is based on the facts that in a cloud-free atmosphere the direct radiation is large, the diffuse radiation is small, and the diurnal variation of the total surface radiation is in accordance with the incoming radiation at the top of the atmosphere. During the SCSMEX IOP, we measured only the total flux but not separately the direct and diffuse components of the radiation. We examined the diurnal variation of the total surface radiation and subjectively identified three days (2 May, 22 May, and 29 June 1998) as being mostly clear. For these three clear days, the total surface radiation (dashed curves in Figure 1) is high and varies smoothly with time, following the radiation at the top of the atmosphere.

When clouds block the sun, the surface radiation is greatly reduced. When clouds do not block the sun but scattered over the observation site, the surface radiation is greater than that of clear skies. Thus, clouds could either increase or decrease the surface radiation depending upon the relative locations of clouds, the sun, and the surface site. These situations can be clearly seen in Figure 1 (dashed curves). To estimate the clear-sky surface downward SW radiation, $F^{\downarrow}$, of those mostly clear days, we make the following adjustments to the measured surface radiation. First, we delete those data which are obviously affected by clouds. For example, the data in the early morning and late afternoon on 2 May (Figure 1a). Second, the remaining data are fit by a third-order polynomial function of the solar zenith angle, μ_o, separately for morning and afternoon data. It is found that $F^{\downarrow}$ varies rather linearly with μ_o, and the third-order polynomial function fits well the surface radiation. Third, we further delete those data that deviate from the regression curves by >15 W m^{-2}. The remaining data are further fit by a third-order polynomial function of μ_o, again separately for morning and afternoon data. Finally, we replace the data deleted in the first and third steps by that computed from the regression curves. The diurnal variations of the reconstructed $F^{\downarrow}$ are shown by the solid curves in Figures 1a-c.

As can be seen in Figures 1a-c, the atmosphere on 29 June is the clearest among the three days. Unfortunately, there were no balloon sounding and sunphotometer measurements, and humidity and aerosol information are not available on that day. After the first surge of the monsoon passing through Dungsha on 10 June 1998, there was nearly no rain on the island, and the standard deviation of the 12-hourly column water vapor amount was only 0.4 cm. Therefore, we use the water-vapor soundings on 22 June

as a surrogate for 29 June. Figure 2 shows the measured downward surface SW fluxes on 29 June and 30 June. Although the cloud effect on the surface radiation is large on 30 June, the two curves overlap very well when there is no cloud interference. It indicates that the AOT is similar on both days. Therefore, we use the average AOT inferred for the morning on 30 June to compute the surface radiation on 29 June.

The AOT measurements on 2 May, 22 May, and 30 June are shown in Figures 3a-c, respectively. The AOT pattern on June 30 (Figure 3c) depends weakly on wavelength, which is quite different from the other two clear days in May (Figures 3a and 3b). The weather before the development of South China Sea summer monsoon was dominated by a quasi-stationary frontal system along the coastline of China. One can expect that fine-sized pollutants transported southerly from China to the South China Sea. When the first transition period of the South China Sea monsoon developed in late May 1998, the weather system was dominated by the prevailing southwesterly wind. It is expected that most of aerosol particles were sea salt but not the anthropogenic sulfuric aerosols from China. The weak dependence of AOT on wavelength shown in Figure 3c is related to the large sea salt particles. Furthermore, the AOT of the maritime aerosols is much smaller than that of the continental aerosols (Figures 3a and 3b).

In computing fluxes, we divide the atmosphere into 75 vertical layers. The thickness of a layer in the troposphere is ~25 hPa. The radiosoundings of atmospheric temperature and humidity taken at 0600 UTC are used to represent the daytime conditions. Fluxes are computed at 1-min resolution. Information on the vertical distributions of aerosols and column-integrated ozone amount are not available for flux calculations. Therefore, we assume that aerosol optical thickness derived from the

CIMEL sunphotometric measurement has a uniform vertical distribution below the 800-hPa level. Sensitivity tests show that the results are not sensitive to the assumed thickness of the aerosol layer. For an aerosol optical thickness < 0.3 at the visible spectral region, the daily-mean downward surface flux changes by only <0.5 W m^{-2} when the top of the aerosol layer is extended from the 800 hPa to 600 hPa. The surface SW fluxes are also not sensitive to the ozone amount. For a change of the ozone amount from 0.30 $(cm\text{-}atm)_{stp}$ to 0.35 $(cm\text{-}atm)_{stp}$, the daily-mean surface SW flux reduces by <0.5 W m^{-2}. Therefore, we use an ozone profile typical of a midlatitude summer atmosphere, which has an column amount of 0.32 $(cm\text{-}atm)_{stp}$, in all calculations.

Figure 4 shows diurnal variations of the incoming solar flux at the top of the atmosphere (upper curves), the reconstructed (dashed curves) and the model-calculated (solid curves) $F^{\downarrow}$. Diurnal distributions of the difference between the reconstructed and the calculated $F^{\downarrow}$ are shown in Figure 5. The large difference in the early morning and the late afternoon on 2 May is due to the extrapolation of the clear-sky flux to these hours when the sky was cloudy, as indicated in the measured surface flux shown in Figure 1a (dashed curve). The relatively large bias of the model-calculated $F^{\downarrow}$ on 29 June is due primarily to the lack of direct information on water vapor and aerosols. Table 1 summarizes the water vapor amount and the aerosol optical thickness used in the radiation model calculations, as well as the incoming SW flux at the top of the atmosphere, surface measurements, and model calculations. The daily-mean difference between the reconstructed and the model-calculated $F^{\downarrow}$ is 1.2, 0.9, and 7.1 Wm^{-2} for 2 May, 22 May, and 29 June, respectively.

4. Conclusion

During the SCSMEX Intensive Observing Period, which covers 50 days in May and June 1998, only three days are found to be clear with minimal cloudiness at Dungsha. Diurnal cycles of the clear-sky surface downward SW flux, $F^{\downarrow}$, are reconstructed by removing the effect of clouds based on the near-linear relationship between $F^{\downarrow}$ and the cosine of the solar zenith angle. The reconstructed $F^{\downarrow}$ on the three clear days are compared with radiative transfer model calculations. The input data to the model calculations include the temperature and humidity profiles from radiosoundings and the aerosol optical thickness inferred from sunphotometric radiance measurements. The difference between the measured and the model-calculated $F^{\downarrow}$ is <3% of the daily means, which is comparable to the estimated uncertainty of the surface measurements. The result is consistent with a previous study using TOGA CAORE measurements, which found good agreement between observations and model calculations. Averaged over the three clear days, $F^{\downarrow}$ is 314 Wm^{-2} from observations and 317 Wm^{-2} from model calculations.

Previous studies on $F^{\downarrow}$ by other investigators gave mixed results. Some showed good agreement between model-calculated and measured $F^{\downarrow}$. Others showed significant disagreement. Those studies covered different geographic locations in the tropical western Pacific and the ARM sites. Whether radiative transfer models overestimate the surface radiation, or equivalently underestimate the atmospheric absorption, is likely to remain an issue for some time to come. The results of this study provide an extra piece of useful information on the modeling of radiative transfer in a clear-sky atmosphere, which fills in the puzzle of the absorption of solar radiation in the atmosphere.

Acknowledgment. The work conducted at the National Taiwan University was supported by National Science Council in Taiwan. The work conducted at NASA Goddard Space Flight Center was supported by the Radiation Processes Program, NASA Office of Earth Science. The NASA Aeronet group processed the Cimel data. Prof. Pay-Liam Lin of National Central University, Taiwan, provided the ISS data set, and the Dungsha Weather Station, Naval Meteorological Center, Taiwan, provided logistic support.

References

Arking, A., Absorption of solar energy in the atmosphere: discrepancy between model and observations, *Science*, *273*, 779-792, 1996.

Arking, A., The influence of clouds and water vapor on atmospheric absorption, *Geophys. Res. Lett.*, *26*, 2729-2732, 1999.

Cess, R. D., M. H. Zhang, P. Minnis, L. Corsetti, E. G. Dutton, B. W. Forgan, D. P. Garber, W. L. Gates, J. J. Hack, E. F. Harrison, X. Jing, J. T. Kiehl, C. N. Long, J.-J. Morcrette, G. L. Potter, V. Ramanathan, B. Subasilar, C. H. Whitlock, D. F. Young and Y. Zhou, Absorption of solar radiation by clouds: Observations versus models, *Science*, *267*, 496-499, 1995.

Chou, M. D., and W. Zhao, Estimation and model validation of surface shortwave radiation and cloud radiative forcing using TOGA COARE measurements, *J. Climate*, *10*, 611-620, 1997.

Chou, M. D., and M. J. Suraez, A shortwave radiation Parameterization for atmospheric studies. *Volume 15, Technical Report Series on Global Modeling and Data Assimilation*, NASA/TM-1999-104606. pp40, 1999.

Conant, W. C., A. M. Vogelmann and V. Ramanathan, The unexplained solar absorption and atmospheric H_2O: a direct test using clear-sky data, *Tellus*, *50A*, 525-533, 1998.

Fu, Q., G. Lesins, J. Higgins, T. Charlock, P. Chylek and J. Michalsky, Broadband water vapor absorption of solar radiation tested using ARM data. *Geophy. Res. Letter*, *25*, 1169-1172, 1998.

Halthore, R. N., S. Nemesure, S. E. Schwartz, D. G. Imre, A. Berk, E. G. Dutton and M. H. Bergin, Models overestimate diffuse clear-sky surface irradiance: A case for excess atmospheric absortpion. *Geophy. Res. Let.*, *25*, 3591-3594, 1998.

Holben, N. L., T. F. Eck, I. Slutker, D. Tanre, J. P. Buis, A. Setzer, E. Vermote, J. A. Reagan, Y. J. Kaukman, T. Nakajima, F. Lavenu, I. Jankowiak and A. Smirnov, AERONET - a federated instrument network and data archive for aerosol characterization. *Remote Sens. Enviorn.*, *66*, 1-16, 1998.

Imre, D. G., E. H. Abramson, and P. H. Daum, Quantifying cloud-induced shortwave absorption: An examination of uncertainties and of recent arguments for large excess absorption, *J. Appl. Meteorol.*, 35, 1991-2010, 1996.

Ji, Q. and S. C. Tsay, On the dome effect of Epply Pyrgeometers and Epply Pyranometers, *J. Geophys. Res.*, 2000.

Kato, S., T. P. Ackerman, E. E. Clothiaux, J. H. Mather, G. G. Mace, M. L. Wesely, F. Murcray and J. Michalsky, Uncertainties in modeled and measured clear-sky surface shortwave irradiances. *J. Geophy. Res.*, *27*, 25881-25898, 1997.

Lau, K. M., Y. Ding, J. T. Wang, R. Johnson, T. Keenan, R. Cifelli, J. Gerlach, O. Thiele, T. Rickenbach, S. C. Tsay and P. H. Lin, A report of the field operations and early results of the South China Sea Monsoon Experiment (SCSMEX). *Bull. Amer. Meteor. Soc.*, xxxx-xxxx, 2000.

Li, Z., L. Moreau and A. Arking, On solar energy disposition: a perspective from observation and modeling, *Bull. Amer. Meteor. Soc.*,*78*, 53-70, 1997.

Mlawer, E. J., P. D. Brown and S. A. Clough, Comparison of spectral direct and diffuse solar irradiance measurements and calculations for cloud-free conditions, *Geophy. Res. Letter*, 2000. submitted.

Pilewskie P., F. P. J. Valero, Direct observations of excess solar absorption by clouds, *Science*, *267*, 1626-1629, 1995.

Pilewskie, P., M. Rabbette, R. Bergstrom, J. Marquez, B. Schmid, and P. B. Russell, The discrepancy between measured and modeled downwelling solar irradiance at the ground: Dependence on water vapor. *Geophy. Res. Lett*, *27*, 137-140, 2000.

Ramanathan, V., B. Subasilar, G. J. Zhang, W. Conant, R. D. Cess, J. T. Kiehl, H. Grassl, and L. Shi, Warm pool heat budget and shortwave cloud forcing: A missing physics? *Science*, *267*, 499-503, 1995.

Wentz, F. J., *User's Manual SSM/I -2 Geophysical Tapes. Tech. Rep.* 070194, 20 pp, 1994. [Available from Remote Sensing Systems, Santa Rosa, CA.]

Table 1. Daily mean values of the column water vapor (w), aerosol optical thickness in the UV (τ_{uv}), visible (τ_v), and infrared (τ_{ir}) spectral regions, insolation at the top of the atmosphere (S_{toa}), reconstructed surface downward SW flux ($F^{\downarrow}_r$), mean atmospheric transmittance (T), and model-calculated surface downward SW flux ($F^{\downarrow}_m$).

	May 2	May 22	June 29
w (cm)	5.6	5.9	5.6
τ_{uv}	0.45	0.42	0.09
τ_v	0.27	0.27	0.06
τ_{ir}	0.10	0.13	0.04
S_{toa} (W m^{-2})	450.6	457.5	458.7
$F^{\downarrow}_r$ (W m^{-2})	308.1	312.6	319.7
T (%)	68.4	68.3	69.7
$F^{\downarrow}_m$ (W m^{-2})	309.3	313.5	326.8

Figure Captions:

Figure 1: Diurnal variations of the measured surface downward SW flux (dashed curve), and the reconstructed clear-sky downward SW flux (solid curve).

Figure 2: Diurnal variations of the surface downward SW flux measured on 29 June (solid curve) and 30 June (dashed curve) 1998 at Dungsha.

Figure 3: Diurnal variations of the aerosol optical thickness at 340, 500, and 1020 nm measured (retrieved) at Dungsha on 2 May (a), 22 May (b), and 29 June (c) 1998.

Figure 4: Diurnal variations of the insolation at the top of atmosphere (circle-dashed curve), the model-calculated (solid curve) and the reconstructed (dashed curves) surface downward SW fluxes.

Figure 5: Model-calculated surface downward flux minus reconstructed surface downward flux.

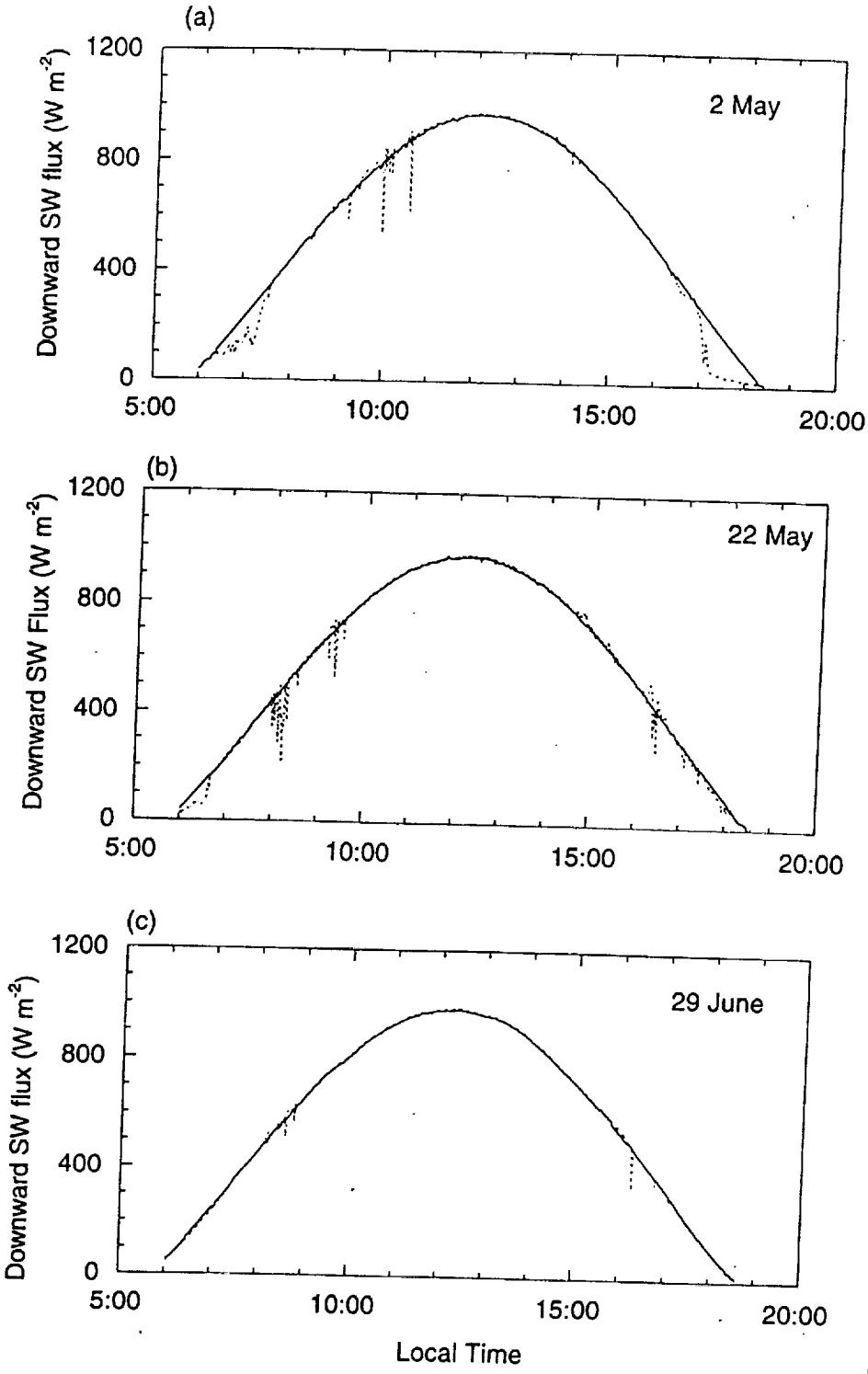
(a)
Downward SW flux (W m-2)
1200
800
400
0
5:00
10:00
15:00
20:00
2 May
(b)
Downward SW Flux (W m-2)
1200
800
400
0
5:00
10:00
15:00
20:00
22 May
(c)
Downward SW flux (W m-2)
1200
800
400
0
5:00
10:00
15:00
20:00
29 June
Local Time

Fig. 1

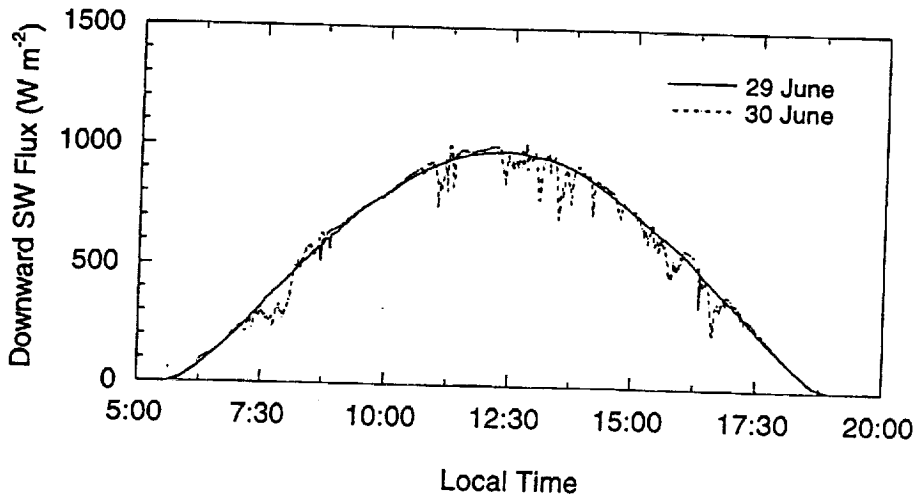
Downward SW Flux (W m-2)
1500
1000
500
0
5:00
7:30
10:00
12:30
15:00
17:30
20:00
Local Time
29 June
30 June

Fig. 2

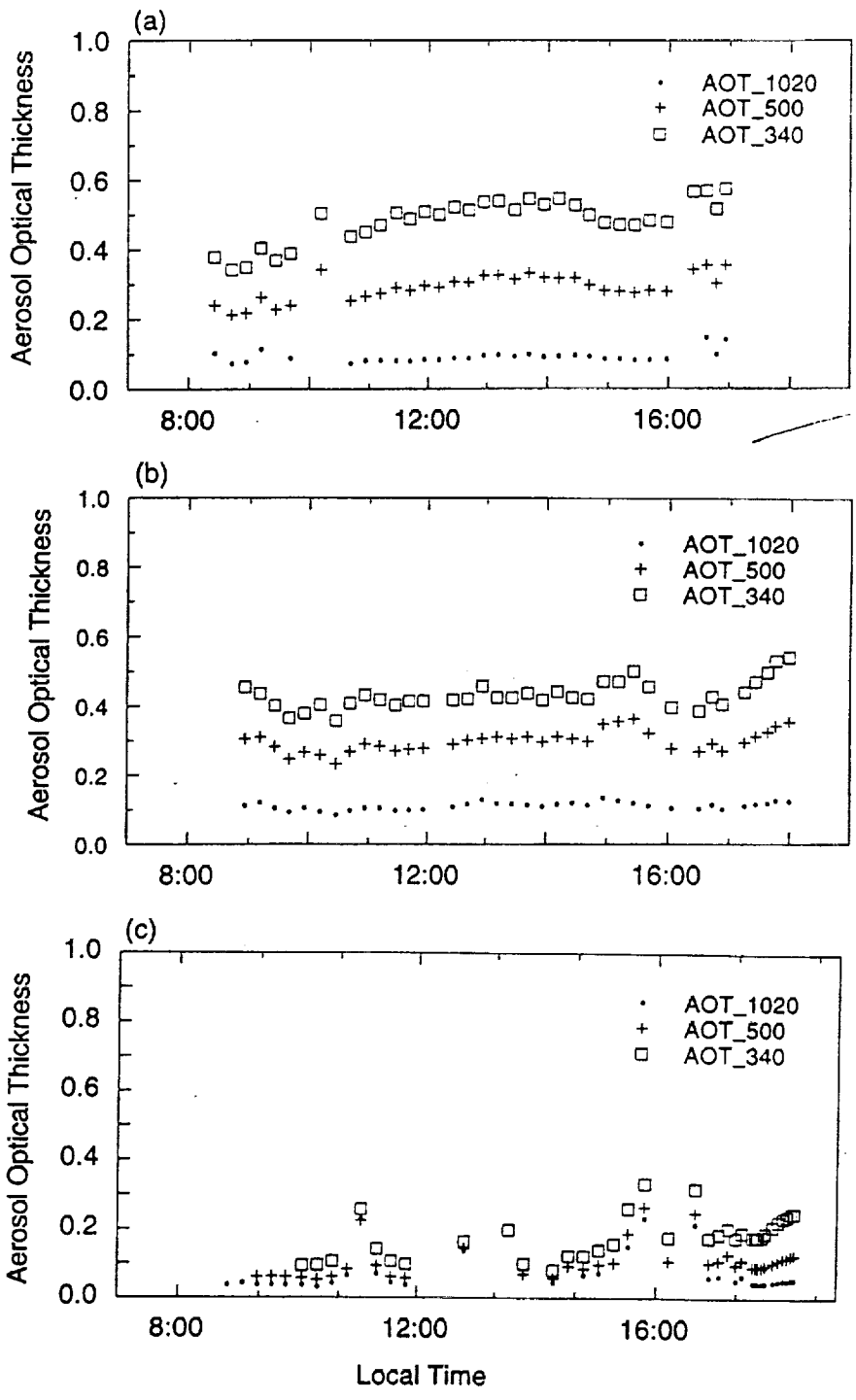
(a)
Aerosol Optical Thickness
1.0
0.8
0.6
0.4
0.2
0.0
AOT_1020
AOT_500
AOT_340
8:00
12:00
16:00
(b)
Aerosol Optical Thickness
1.0
0.8
0.6
0.4
0.2
0.0
AOT_1020
AOT_500
AOT_340
8:00
12:00
16:00
(c)
Aerosol Optical Thickness
1.0
0.8
0.6
0.4
0.2
0.0
AOT_1020
AOT_500
AOT_340
8:00
12:00
16:00
Local Time

Fig 3

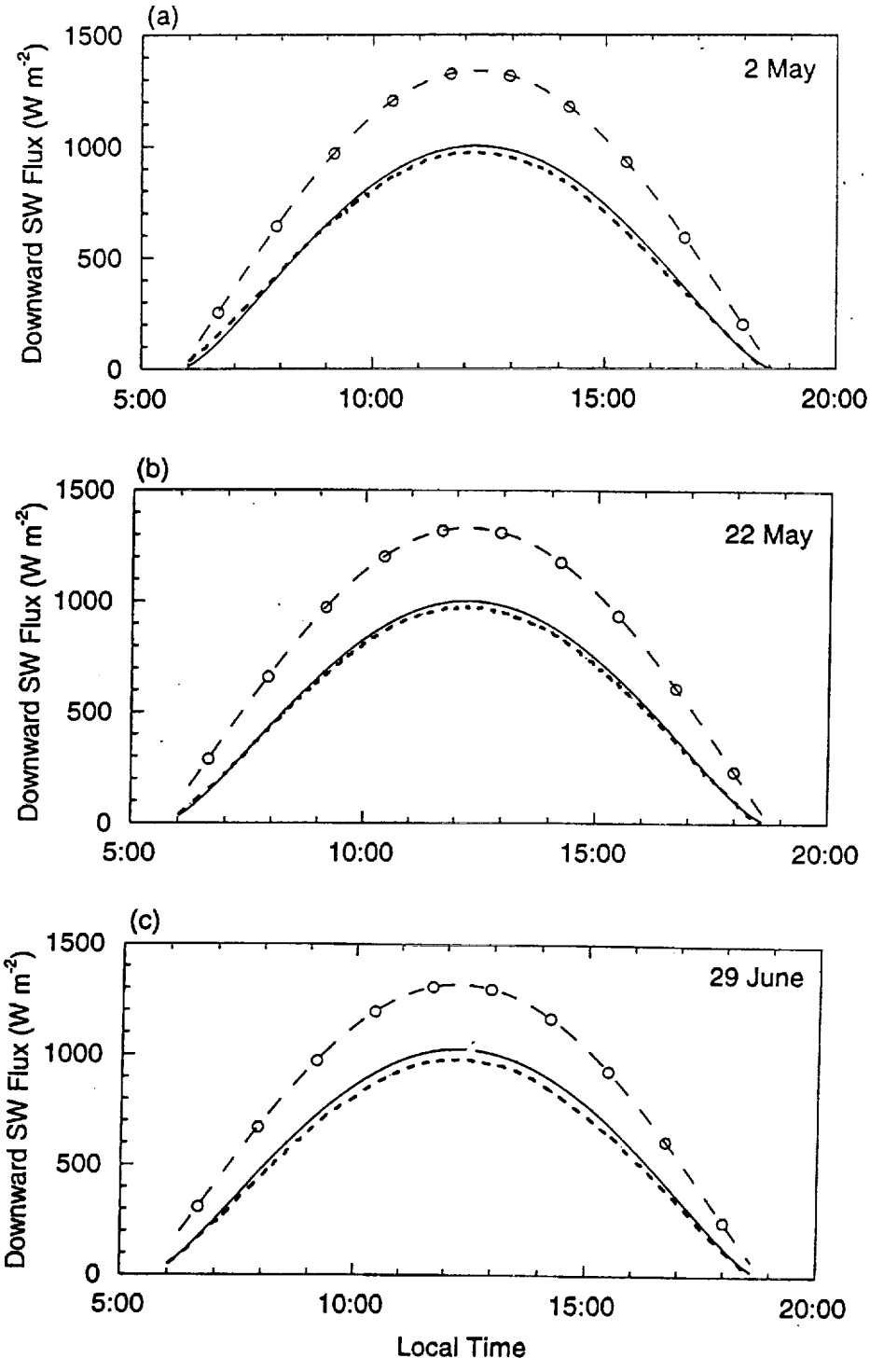
(a)
2 May
(b)
22 May
(c)
29 June
Downward SW Flux (W m-2)
1500
1000
500
0
5:00
10:00
15:00
20:00
Local Time

Fig. 4

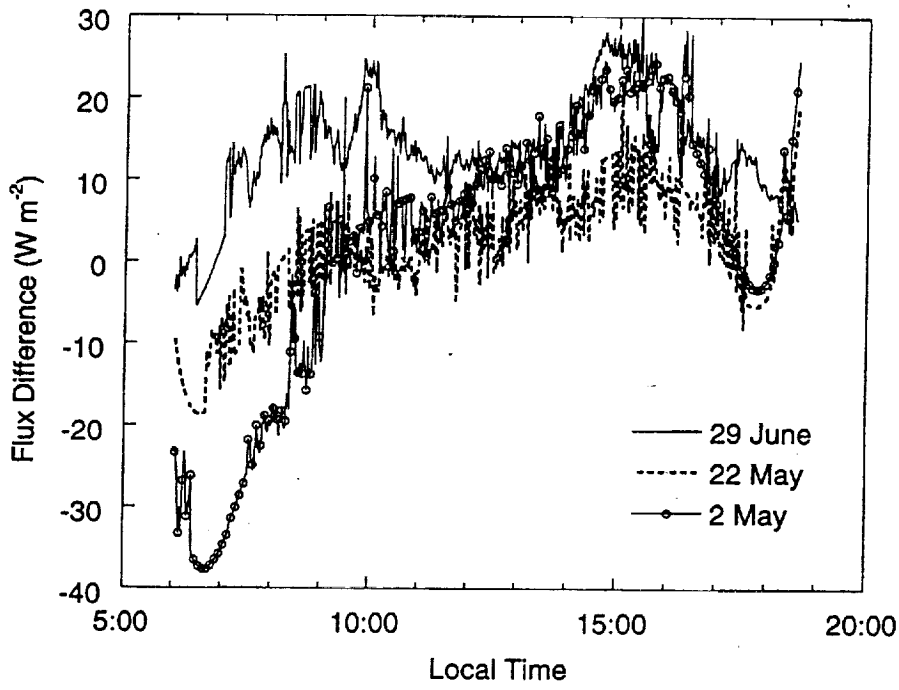
30
20
10
0
-10
-20
-30
-40
Flux Difference (W m-2)
5:00
10:00
15:00
20:00
Local Time
29 June
22 May
2 May

Fig. 5